LAMINAR CIRCULAR ENTRY FLOWS OF VISCOELASTIC FLUIDS

R.J. BINNINGTON and D.V. BOGER

Department of Chemical Engineering
University of Melbourne, Parkville, Vic. 3052
AUSTRALIA

ABSTRACT

Understanding the kinematics of viscoelastic fluids in entry flows continues to be of importance in most fluid processing operations. It is shown in this work that the lip and corner vorticies encountered in contraction flows can exist in isolation from each other, or in a figure-eight combination of both. A probable mechanism is proposed for the vortex interaction based on the influence of an extensionally formed, solid-like core of viscoelastic fluid at the entry zone. This postulate is tested using a purely Newtonian simulation, experimentally and numerically, in a re-entrant tube entry flow geometry.

INTRODUCTION

The laminar entry flow field for Newtonian and inelastic fluids is now well understood, both for low Reynolds number flows and for higher Reynolds number flows where inertial forces become significant below the transition to turbulence (see Boger (1987), Kim-E et al (1983)). A current challenge in non-Newtonian fluid mechanics is to solve non-viscometric flow problems for viscoelastic fluids with a significant elongational component. The most appropriate test geometry used in developing numerical simulation techniques and constitutive equations to model real flow kinematics is a circular contraction geometry. Observations are presented on the kinematics of a non-shear thinning elastic fluid in an abrupt 4 to 1 and a 22 to 1 contraction. To gain some insight into understanding the mechanism of the kinematics observed for contraction flows of viscoelastic fluids, a series of Newtonian flow simulations in a re-entrant tube geometry are compared to experimental observations.

The most recent numerical simulation results for viscoelastic fluids in contraction flows are summarised in publications by Dupont and Crochet (1988) and Debbaut et al (1988). A review by White et al (1987) provides information on the behaviour of polymers in entry flows while the experimental observations and results of Evans and Walters (1989), Piau et al (1988) and Raiford et al (1989) are of immediate interest.

RESULTS AND DISCUSSION

Flow Visualisation

The test fluid (fluid M1) used in these investigations is a solution of polyisobutylene in a base solvent of polybutene and kerosene which has the basic characteristics of a so-called Boger fluid as reported by Boger (1977/78), being optically clear and having essentially a constant viscosity (in this case η = 2.65 Pa.s at 21°C) and a region of second-order normal stress behaviour as shown by the Weissenberg cone-and-plate viscometer data in Figure 1. The Maxwell relaxation time (λ_o) given by

$$\lambda_o = N_1/2\dot{\gamma}^2\eta \qquad (1)$$

in the limit of low shear rate is 0.28 sec for fluid M1.

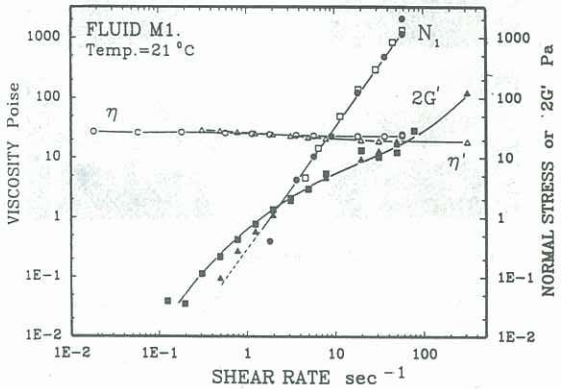

Figure 1: Flow property data for fluid M1.

Techniques of streak photography developed earlier by Nguyen (1978) and (1979) were used to observe the kinematics of the test fluid in abrupt circular contractions of 4 to 1 and 22 to 1 ratios. The upstream flow patterns are characterised by the dimensionless re-attachment length of the secondary vortex (X) where

$$X = L/D_u \qquad (2)$$

L is the length of the cell from the contraction plane to its attachment point on the wall of the upstream tube and D_u is the upstream tube diameter.

It should be noted that for Newtonian (inelastic) fluids there is excellent agreement with respect to the re-attachment length and the shape of the secondary cell between experimental observation and numerical simulation as reported by Boger et al (1986). The cell is concave in shape with respect to the re-entrant corner with a length, X = 0.17, which remains constant until the downstream

Reynolds number, Re, exceeds 0.1, beyond which the cell decreases in size due to fluid inertia.

Of particular interest in circular contracting flows are the more complicated and less readily predicted kinematics encountered with viscoelastic fluids, characterised by secondary flow vorticies which can exist in the form of a single corner vortex, or a lip vortex, or a figure-eight combination of both. The photographs shown in figures 2 and 3 illustrate the various forms of fluid behaviour. The figures are characterised by the cell size, X, downstream shear rate, $\dot{Y}$, downstream Reynolds number, Re = $DV\rho/\mu$, and Weissenberg number We = $\lambda\dot{Y}$ where

$$\dot{Y} = \frac{3n+1}{4n} \left(\frac{8V}{D}\right) \qquad (3)$$

The power law index (n) is 0.98 for fluid M1.

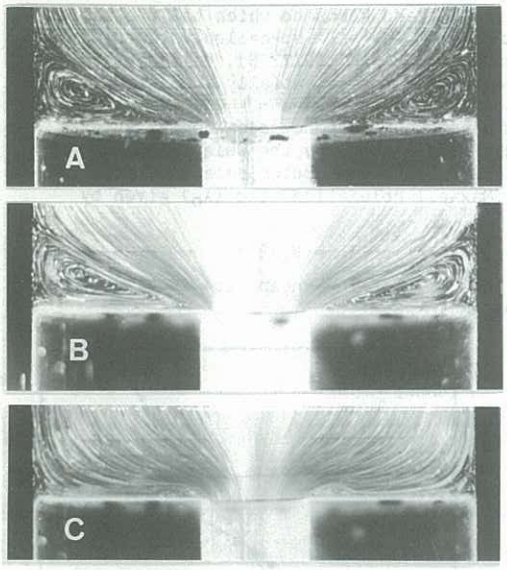

Figure 2: Fluid M1 kinematics in a 4:1 circular contraction (a) Re = 0.009, $\lambda\dot{Y}$ = 0.36, X = 0.175 (b) Re = 0.15, $\lambda\dot{Y}$ = 7.2, X = 0.18 (c) Re = 0.545, $\lambda\dot{Y}$ = 23, X = 0.

Figure 2 demonstrates the transformation of the corner vortex from Newtonian-like shape and size (X = 0.175) in Figure 2a for a contraction ratio of 4:1. As the Reynolds number is increased, the corner vortex boundary straightens, X increases marginally and then begins to decrease under the apparent influence of inertia as shown in Figure 2b where Re = 0.15. Finally, in Figure 2c fluid inertia has 'pushed out' the corner vortex leaving a lip vortex at the contraction entrance. In the absence of significant fluid inertia there is ample evidence in the literature (Evans (1989)) to suggest that the lip vortex would grow with increasing Weissenberg number ($\lambda\dot{Y}$), however in this case, inertia dominates any elastic effects and the vortex does not grow.

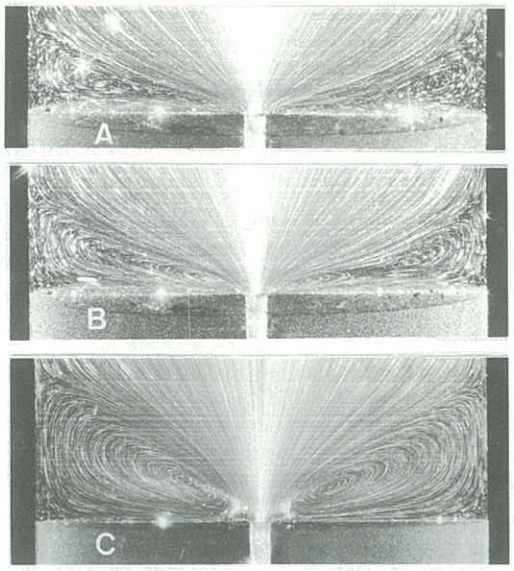

Figure 3: Fluid M1 kinematics in a 22:1 circular contraction (a) Re = 0.003, $\lambda\dot{Y}$ = 4.2, X = 0.18 (b) Re = 0.0054, $\lambda\dot{Y}$ = 7.2, X = 0.195 (c) Re = 0.015, $\lambda\dot{Y}$ = 21, X = 0.31.

Figure 3 shows that entry flow of the same fluid M1 through a 22 to 1 contraction reveals no 'inertial-like' phenomena and significant vortex growth is observed as Reynolds number is increased. Close examination of the photographs reveals a phenomena similar to those reported by Piau et al (1988). The corner vortex begins at a Newtonian cell length (X = 0.175) as in Figure 3a but a lip vortex, which is more evident in Figure 3b, develops and coexists with the corner vortex in a figure-eight formation. The lip vortex grows at the expense of the corner vortex, finally dominating as shown in Figure 3c where X = 0.31.

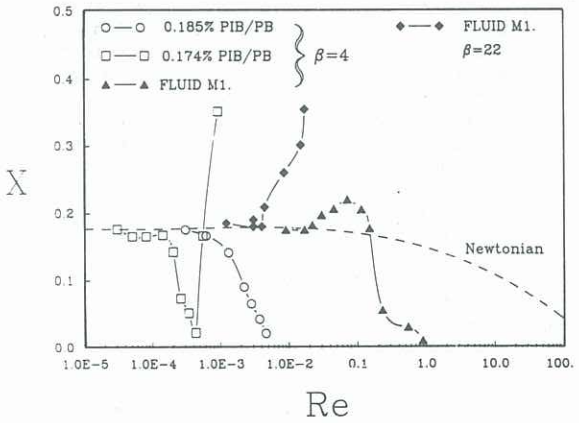

Figure 4: Dimensionless cell size versus Reynolds number for fluid M1 and two other Boger fluids.

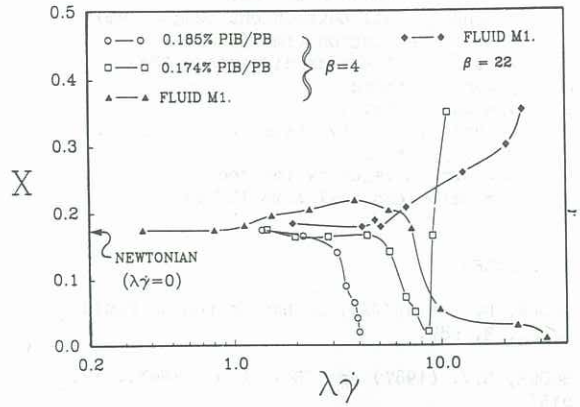

Figure 5: Dimensionless cell size versus Weissenberg number ($\lambda\dot{\gamma}$) for fluid M1 and two other Boger fluids.

Figure 4 shows the cell size characteristics of fluid M1 and two similar Boger fluids as a function of Reynolds number, while Figure 5 shows cell size as a function of $\lambda\dot{\gamma}$. It should be noted that fluid M1 is less viscous and less elastic (η = 2.65 Pa.s, λ_o = 0.28s) than the 0.185% PIB/PB (η = 28.9 Pa.s, λ_o = 0.27s) and the 0.174% PIB/PB (η = 95 Pa.s, λ_o = 1.4s) fluids. It is evident in Figure 4 that the inertial-like reduction in the vortex size (X) is more pronounced and/or occurs at lower Reynolds numbers for elastic liquids than for purely Newtonian liquids. This demonstrates that it is essential that inertial terms are not neglected in the formulation of numerical solutions for elastic liquids. Figure 5 confirms this conclusion by showing that no unique relationship exists between the cell size and the Weissenberg number for these fluids in a 4 to 1 contraction. It appears that a complex interaction exists between inertia and elasticity, including the extensional characteristics, which is not fully understood at this stage as evidenced by the significant differences in observed kinematics for fluids with essentially the "same flow properties" (Boger (1987)).

The observations shown in Figure 3 are the basis of a postulated mechanism for the lip vortex generation and interaction with the corner vortex. It is postulated that because of the high extensional strain and strain rate experienced by an elastic liquid in the acceleration zone of an abrupt contraction, the fluid behaves in a solid-like manner in that zone immediately upstream of the contraction entrance. This solid-like core now blocks flow in from the concave cell-boundary streamline causing the lip vortex to be generated behind this "blockage". As the flow rate is increased this core region extends further upstream ultimately creating the conditions for the 'lip vortex' to consume the original corner vortex and become dominant.

Numerical Simulation of Postulate.

The mechanism proposed above for the generation of a lip vortex was examined using a purely Newtonian fluid in a re-entrant tube geometry as shown in Figure 6. The figure shows the excellent agreement attained between the experimental observations and the numerical predictions using Polyflow (Numerical simulation package by Professor M. Crochet, Belgium).

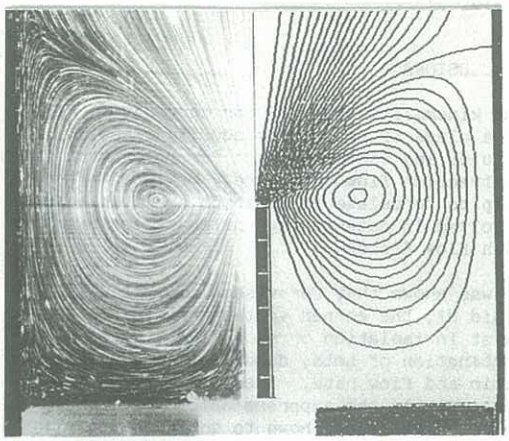

Figure 6: Re-entrant tube flow for a Newtonian fluid experiment compared to Polyflow simulation.

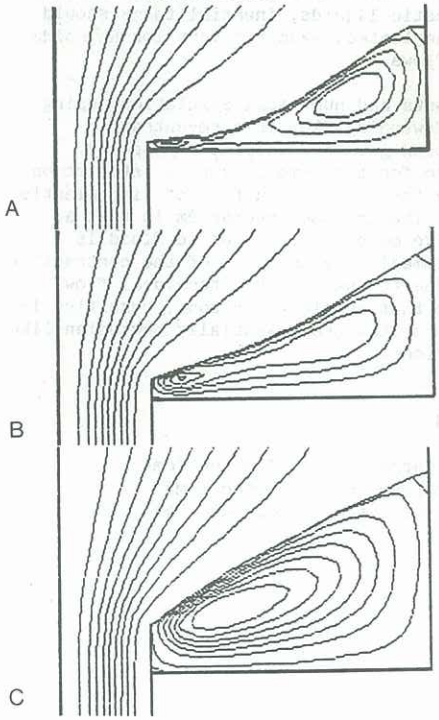

Figure 7: Newtonian simulation in a re-entrant geometry. Re-entrant tube length: (a) 1.75%D_u (b) 3.5%D_u (c) 9%D_u

Figure 7 shows the sequence of Newtonian kinematics resulting from the increasing protrusion of the re-entrant tube into the upstream flow field of a 4 to 1 contraction. The figure-eight combination of the corner and lip vorticies is clearly evident in Figure 7(b). This sequence of events provides quite a logical explanation for the similar kinematics observed for fluid M1 in the 22:1 contraction (see Figure 3), as well as for other elastic fluids in similar accelerating flow fields. If this postulated mechanism is correct, then much of the complex kinematics observed in the contraction flows of viscoelastic fluids could be mainly attributed to Newtonian kinematics which arise as a consequence of extensional phenomena occurring

in the accelerating central core of the flow field.

CONCLUSIONS

The kinematics observed for contraction flow of a class of constant viscosity elastic liquids and those observed for re-entrant tube contraction flow of a purely Newtonian fluid help to formulate ideas about the mechanisms involved in determining the characteristics of such flow fields.

It was shown that for viscoelastic fluids like fluid M1, the corner vortex and lip vortex can exist in isolation or as a figure-eight combination of both, depending on contraction ratio and flow rate. Inertial-like effects, particularly the suppression of the corner vortex, have been shown to dominate the kinematics of such fluids in contraction flows even at Reynolds numbers significantly below where traditional inertial effects are observed for Newtonian fluids. It can thus be concluded that, in the formulation of numerical solutions for contraction flows of viscoelastic liquids, inertial terms should not be neglected, even for very low Reynolds number flows.

Experiments and numerical simulations using purely Newtonian flow in a re-entrant contraction geometry support a proposed mechanism for the complex vortex interaction observed for contraction flow of viscoelastic fluids. The proposed mechanism is that a solid-like core of viscoelastic fluid is formed immediately upstream of the contraction plane, due to the strong extensional flow field in that acceleration zone, resulting in kinematics that are essentially Newtonian-like in behaviour.

NOTATION

D = downstream tube diameter (cm)
D_u = upstream tube diameter (cm)
G' = dynamic storage modulus (Pa)
$\dot{\gamma}$ = downstream shear rate (sec^{-1})
L = secondary cell dettachment length (cm)
λ_o = Maxwell relaxation time (sec)
N_1 = first normal stress difference (Pa)
n = power law index
η = viscosity (Pa.s)
η' = dynamic viscosity (Pa.s)
ρ = density (gm/cc)
V = downstream velocity (cm/sec)
X = dimensionless cell size (L/Du)

REFERENCES

BOGER, D.V. (1977/78) J. Non-Newtonian Fluid Mech., 3, p87.

BOGER, D.V. (1987) Ann. Rev. Fluid Mech., 19, p157.

BOGER, D.V., HUR, D.U. and BINNINGTON, R.J. (1986) J. Non-Newtonian Fluid Mech., 20, p31.

COCHRANE, T., WALTERS, K. and WEBSTER, M.F. (1981) Phils-Trans. R. Soc. Lond., A301, p163.

DEBBAUT, B., MARCHAL, J.M. and CROCHET, M.J. (1988) J. Non-Newtonian Fluid Mechanics, 29, p119.

DUPONT, S. and CROCHET, M.J. (1988) J. Non-Newtonian Fluid Mech., 29, p81.

EVANS, R.E. and WALTERS, K. (1989) J. Non-Newtonian Fluid Mech., 32, p95.

KIM-E, M.E., BROWN, R.A. and ARMSTRONG, R.C. (1983) J. Non-Newtonian Fluid Mech., 13, p341.

NGUYEN, T.H. (1978) The Influence of Elasticity on Die Entry Flow, PhD thesis, Monash University, Australia.

NGUYEN, T.H. and BOGER, D.V. (1979) J. Non-Newtonian Fluid Mech., 5. p353.

PIAU, J.M., EL KISSI, N. and TREMBLAY (1988) J. Non-Newtonian Fluid Mech., 30, p197.

WHITE, S.A., GOTSIS, A.D. and BAIRD, D.G. (1987) J. Non-Newtonian Fluid Mech., 24, p121.